The Auger recombination rate is larger in a GaSb quantum well than in bulk GaSb

Y. Jiang, M. C. Teich, and W. I. Wang
Department of Electrical Engineering, Columbia University, New York, New York 10027

(Received 27 July 1990; accepted for publication 10 September 1990)

The band-to-band Auger recombination rate in bulk GaSb and in a GaSb quantum well is calculated. It turns out to be larger in the quantum well because the threshold of the Auger process is located at the band edge where the density of states is larger in the quantum well than in bulk. A simple picture is developed to illustrate the physics of the Auger processes in bulk and quantum-well direct-band-gap semiconductors. With this picture, we propose that the composition-disorder-induced band mixing should be considered in order to explain the unusual behavior of the Auger process in an InGaAsP quantum-well structure.

I. INTRODUCTION

AlGaAs quantum-well (QW) lasers exhibit very low threshold currents. It is generally believed that the quantum size effect of a QW structure should reduce the Auger recombination rate, and therefore the threshold current, of long-wavelength lasers as well.[1] However, InGaAsP QW lasers, which are used in 1.3–1.6-μm lightwave communication systems, have not fulfilled that expectation. There is not much experimental evidence on the question of whether GaSb QW lasers, which are also candidate transmitters for long-wavelength communications, can achieve low threshold currents. The numerical calculation by Sugimura *et al.*[2] indicates a significant reduction in the Auger effect, which therefore suggests that GaSb laser performance should be enhanced by the use of a QW structure.

The reasoning in Ref. 2 is that the effective spin-split-off energy gap Δ increases as the QW width L decreases. This increase of Δ brings it closer to the band-gap energy E_g in an InGaAsP QW, whereas in a GaSb QW, on the other hand, it brings it away from E_g because it is already comparable to E_g in the bulk material. Because the Auger recombination rate peaks in semiconductors for which Δ is near E_g, the reasoning goes that InGaAsP QWs should show an increase, and GaSb QWs should show a decrease, in the Auger recombination rate as the well width L decreases.

In fact, in direct-band-gap semiconductor QWs, the increase in the effective band gap is greater than that of the effective spin-split-off gap because the effective mass in the conduction band is smaller than the effective mass in the spin-split-off band. Therefore, a more sophisticated model is required to explain the discrepancy in the Auger recombination rates in bulk and QW structures. We have developed such a model and calculated the Auger recombination rates in bulk and QW GaSb structures; our results show that the rate in a GaSb QW is greater than that in the bulk material. We also have developed a simple picture to illustrate the physics of the Auger processes in bulk and QW direct-band-gap semiconductors. This picture can be used to explain qualitatively the unusual behavior of the Auger processes in an InGaAsP QW structure.

II. FORMULATION

A. *CHHS* Auger recombination in bulk material

Band-to-band Auger recombination in bulk GaSb is dominated by the *CHHS* process, in which a conduction-band electron 1′ (C) recombines with a heavy hole 1 (H) and excites a heavy hole 2 (H) to the spin-split-off band at 2′ (S), as shown in Fig. 1.

The *CHHS* Auger recombination rate R ($\mathrm{cm}^{-3}\,\mathrm{s}^{-1}$) is[3]

$$R = \frac{2\pi}{\hbar}\left(\frac{1}{8\pi^3}\right)^3 \int\int\int\int d^3k_1\, d^3k_2\, d^3k_{1'}\, d^3k_{2'} \times |M|^2 P(1,1',2,2')\delta(\mathbf{k}_1 + \mathbf{k}_2 - \mathbf{k}_{1'} - \mathbf{k}_{2'})\delta(E_i - E_f), \quad (1)$$

where k is the wave vector, E_i is the energy of the initial state,

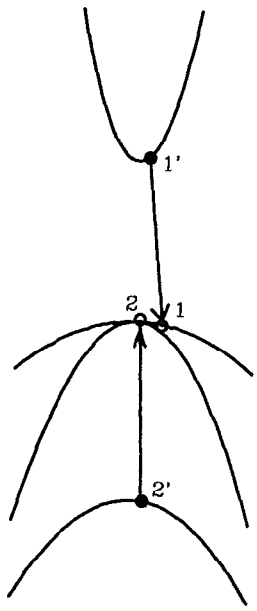

FIG. 1. *CHHS* Auger process.

 0021-8979/91/020836-05$03.00 © 1991 American Institute of Physics

Downloaded 27 Jan 2002 to 168.122.159.57. Redistribution subject to AIP license or copyright, see http://ojps.aip.org/japo/japcr.jsp

E_f is the energy of the final state, and

$$E_i - E_f = E(1') + E(2') - E(1) - E(2). \quad (2)$$

Neglecting exchange terms, the matrix element M is given by

$$|M|^2 = 4\left(\frac{4\pi q^2}{\epsilon}\right)^2 \left|\frac{F_{1,1'}F_{2,2'}}{(\mathbf{k}_{2'} - \mathbf{k}_2)^2 + \lambda^2}\right|^2, \quad (3)$$

where q, ϵ and λ are, respectively, the electron charge, the dielectric constant, and the screening factor, and the $|F_{i,j}|^2$ are the overlap functions.[4] The quantity $P(1,1',2,2')$, taking the reverse process of *CHHS* Auger recombination into account also, represents the occupation probabilities. Assuming that the electron and hole distributions f_n and f_p can be expressed as Fermi distributions, with electron and hole equilibrium Fermi levels F_n and F_p, we have

$$\begin{aligned} P(1,1',2,2') &= f_p(\mathbf{k}_1)f_p(\mathbf{k}_2)f_n(\mathbf{k}_{1'}) \\ &\quad \times [1 - f_p(\mathbf{k}_{2'})] - [1 - f_p(\mathbf{k}_1)] \\ &\quad \times [1 - f_p(\mathbf{k}_2)][1 - f_n(\mathbf{k}_{1'})]f_p(\mathbf{k}_{2'}) \\ &= \{1 - \exp[-(F_n - F_p)/k_B T]\}f_p(\mathbf{k}_1) \\ &\quad \times f_p(\mathbf{k}_2)f_n(\mathbf{k}_{1'})[1 - f_p(\mathbf{k}_{2'})], \end{aligned} \quad (4)$$

where k_B is the Boltzmann constant and T is the temperature. Since the spin-split-off gap $\Delta \gg k_B T$, $f_p(\mathbf{k}_{2'})$ in Eq. (4) can be taken as zero. When $P(1,1',2,2')$ is positive the Auger recombination process dominates, whereas when $P(1,1',2,2')$ is negative the reverse process, impact ionization, dominates.

Although the integrations in Eq. (1) extend over all the values of the wave vectors, they are actually limited by the conservation of energy and momentum. The lowest permissible value of excited hole energy $-E_{2'}$ is called the threshold energy of the Auger recombination E_{th}. $P(1,1',2,2')$ is maximum at the threshold.

We assume that the energy bands are parabolic and denote m_c, m_h, and m_s as the electron, heavy-hole, light-hole, and spin-split-off-hole effective masses, respectively. Defining the new variables

$$\mathbf{p} = \mathbf{k}_{1'} - \mathbf{k}_1 = \mathbf{k}_2 - \mathbf{k}_{2'}, \quad (5)$$

$$\mathbf{K}_1 = \mathbf{k}_{1'} - \frac{\mathbf{p}}{[(m_h/m_c) + 1]}, \quad (6)$$

and

$$\mathbf{K}_2 = \mathbf{k}_{2'} - \frac{\mathbf{p}}{[(m_h/m_s) - 1]}, \quad (7)$$

simplifies the integration in Eq. (1). The δ function for momentum conservation reduces the twelfth-order integration in Eq. (1) to ninth order. Using the same overlap functions as those used in Refs. 3 and 4, in which $|M|$ is a function of p and $k_{2'}$ only, one finds

$$\begin{aligned} R &= \frac{2\pi}{\hbar}\left(\frac{1}{8\pi^3}\right)^3 \\ &\quad \times \int\int\int d^3p\, d^3K_2\, d\Omega_1\, |M|^2 \\ &\quad \times P(1,1',2,2')\frac{K_1}{(h^2/m_h)[(m_h/m_c) + 1]} \\ &= \frac{2\pi}{\hbar}\left(\frac{1}{8\pi^3}\right)^3 4\pi \int p^2\, dp \int K_2^2\, dK_2\, P(1,1',2,2') \\ &\quad \times \frac{K_1}{(h^2/m_h)[(m_h/m_c) + 1]} \\ &\quad \times \left(2\pi \int_0^\pi d\cos\theta_1 f_p(k_1) f_n(k_{1'})\right) \\ &\quad \times \left(2\pi \int_0^\pi d\cos\theta_2 f_p(k_2)|M|^2\right), \end{aligned} \quad (8)$$

where Ω_1 is the solid angle in $\mathbf{K}_1$ space, and θ_1 and θ_2 are, respectively, the angles of $\mathbf{K}_1$ and $\mathbf{K}_2$ with respect to $\mathbf{p}$. The integration over θ_1 can be carried out analytically so that Eq. (8) reduces to a third-order integration.

It is important to note that $|M|$ has poles at $p = 0$ if we assume that the screening factor λ is zero. In some processes, this singularity is cancelled or reduced to a lower order by the zeros at $p = 0$ of the overlap functions and the density of states. For materials like GaSb, which has $p = 0$ at the threshold, the integration near this point is crucial and approximations[2,5] may lead to false results. For Auger processes that have p far from zero at the threshold, on the other hand, the integrations do not include the poles and $|M|$ can be taken to be constant to simplify the calculation.[4]

If the Fermi levels are sufficiently away from the band edges, Eq. (8) can be approximated as

$$R = Cnp^2, \quad (9)$$

where n and p are the electron and hole concentrations, respectively, and the constant C is called the Auger recombination constant. For intrinsic semiconductors, and for semiconductors with high levels of carrier injection, which is the case in semiconductor lasers, $n = p$. The Auger recombination lifetime, defined as

$$\tau = n/R, \quad (10)$$

is a measure that is often used to characterize the performance of semiconductor lasers.

B. *CHHS* Auger recombination in a quantum well

The state of the carriers in the ith band of a quantum well of width L with infinite barriers can be written as[6]

$$\phi_{i,m} = u_{i,\mathbf{k}}(\mathbf{r})e^{-\mathbf{k}\cdot\mathbf{r}_t}\sqrt{(2/L)}\sin(\xi_m z), \quad (11)$$

where u is the periodic part of the Bloch function, $\mathbf{k}$ and $\mathbf{r}_t$ are two-dimensional vectors perpendicular to the width of the well, and

$$\xi_m = m(\pi/L), \quad m = 1,2,\ldots. \quad (12)$$

In analogy with the three-dimensional expression in Eq. (1), the two-dimensional *CHHS* Auger recombination rate per unit volume is

$$\begin{aligned} R &= \frac{2\pi}{\hbar}\left(\frac{1}{4\pi^2}\right)^3 \frac{1}{L^3} \\ &\quad \times \sum_{\xi,\xi_1,\xi_{1'},\xi_2,\xi_{2'}} \int\int\int\int d^2k_1\, d^2k_2\, d^2k_{1'}\, d^2k_{2'}\, |M|^2 \\ &\quad \times P(1,1',2,2')\delta(\mathbf{k}_1 + \mathbf{k}_2 - \mathbf{k}_{1'} - \mathbf{k}_{2'})\delta(E_i - E_f). \end{aligned} \quad (13)$$

Downloaded 27 Jan 2002 to 168.122.159.57. Redistribution subject to AIP license or copyright, see http://ojps.aip.org/japo/japcr.jsp

However, unlike the case of bulk material, the matrix element is now

$$|M|^2 = 4\left(\frac{4\pi q^2}{\epsilon}\right)^2 \left| \frac{F_{1,1'}F_{2,2'}G_{1,1'}(\xi)G_{2,2'}(-\xi)}{(\mathbf{k}_{2'}-\mathbf{k}_2)^2+\xi^2} \right|^2, \quad (14)$$

where

$$G_{i,j}(\xi) = \tfrac{1}{2}(\delta_{\xi,\xi_1-\xi_2} + \delta_{\xi,-\xi_1+\xi_2} - \delta_{\xi,\xi_1+\xi_2} - \delta_{\xi,-\xi_1-\xi_2}). \quad (15)$$

The integrals over the k_z's in Eq. (1) for bulk material become summations over the ξ's for quantum-well structures. The $G_{ij}(\xi)$'s impose selection rules on the summations. Equation (13) can therefore be reduced to an integration of third order, which is similar to Eq. (8).

III. RESULTS AND DISCUSSION

From Eqs. (8) and (13) we can see that the Auger recombination rate is determined by the matrix element $|M|$, the joint occupation distribution $P(1,1',2,2')$, and the density of states. The joint occupation distribution $P(1,1',2,2')$ and the density of states are too complex to be illustrated in a two-dimensional figure. However, some of their features can be illustrated by means of the single-carrier density of states and the occupation distribution. Figure 2 shows the density of states in bulk and QW structures, and the Fermi distribution, for a single carrier and parabolic bands. The density of states in a quantum well is steplike and always lies at or below that of the bulk. The Fermi distribution has an exponential tail for energies sufficiently above the Fermi level. Figure 3 illustrates the product of the density of states and the occupation distribution, which is the carrier population distribution, for two typical threshold energy positions, at and above the band edges, in both bulk and QW structures. Depending on the position of the threshold energy with respect to the band edge, a QW structure will have a greater or lesser amount of Auger recombination in comparison with bulk material.

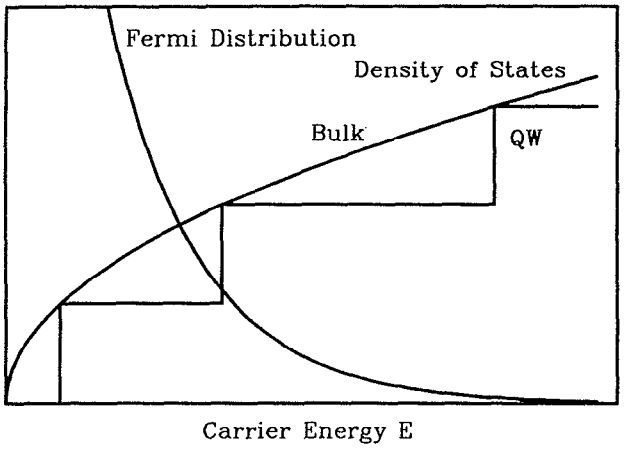

FIG. 2. Carrier occupation distribution (Fermi distribution) and density of states in a bulk and a QW structure with parabolic bands.

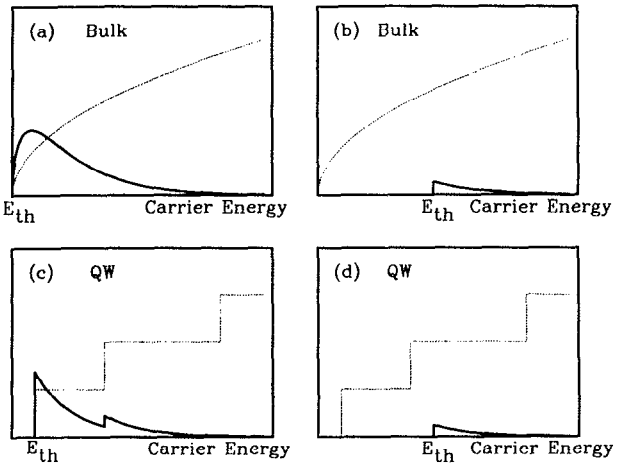

FIG. 3. Density of states (dashed curves) and carrier population distributions (solid curves) in bulk [(a) and (b)] and QW [(c) and (d)] structures. The thresholds are at the band edges in (a) and (c). The thresholds are above the band edges in (b) and (d).

A. Threshold energy at the band edge

The illustrations in Figs. 3(a) and 3(c) apply, respectively, to the *CHHS* process in GaSb bulk and QW structures. The energy thresholds for the Auger process E_{th} are at the band edges. The density of states at threshold is zero for the bulk but not for the QW structure. The Auger recombination rate in a GaSb QW should therefore be greater than that in bulk GaSb. Indeed, the results of our numerical calculation based on Eq. (8) and a simplified version of Eq. (13) confirm this (Fig. 4). The decrease in Auger lifetime with decreasing well width is a result of the increase in the density of states at the threshold.

Figures 5 and 6 show the calculated Auger lifetime in bulk GaSb and in a GaSb QW, respectively, at various values of the temperature. The Auger lifetime in a GaSb QW is less sensitive to temperature than in the bulk material. This is because the maximum value of the product of the joint density of states and the occupation distribution P of the bulk material lies above the threshold energy E_{th} [Fig. 3(a)] and varies with temperature. On the other hand, the maximum for the QW structure is at the threshold [Fig. 3(c)] and does not vary with temperature.

B. Threshold energy above the band edge

The illustration in Fig. 3(b) applies to the *CCCH* Auger process, in which a conduction-band electron 1 (C) recombines with a heavy hole 1′ (H) and excites an electron 2 (C) to a higher-energy state 2′ (C). This is the dominant Auger process in bulk GaAs and HgCdTe when the band gap is compositionally tuned in the mid-infrared region. Figure 3(d) applies to the *CCCH* Auger process in QW structures, such as the GaAs QW, the InGaAs/GaAs strained QW, and the mid-infrared HgCdTe QW. The threshold energies in *CCCH* Auger processes are always above the band edges

Downloaded 27 Jan 2002 to 168.122.159.57. Redistribution subject to AIP license or copyright, see http://ojps.aip.org/japo/japcr.jsp

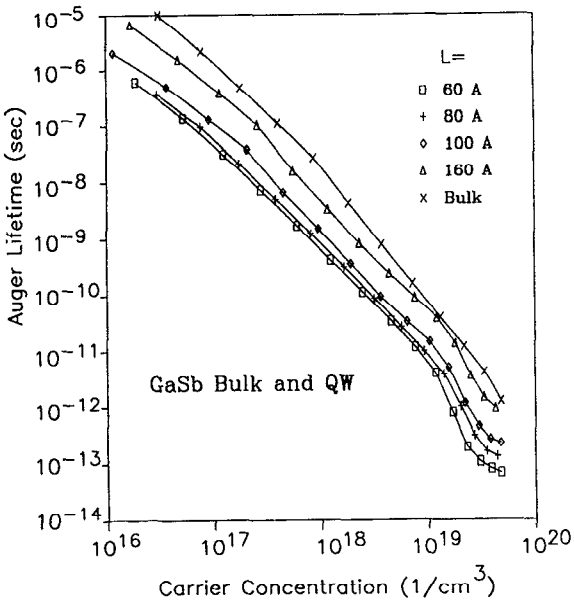

FIG. 4. Calculated band-to-band Auger recombination lifetime in bulk and QW GaSb for different values of the well width L.

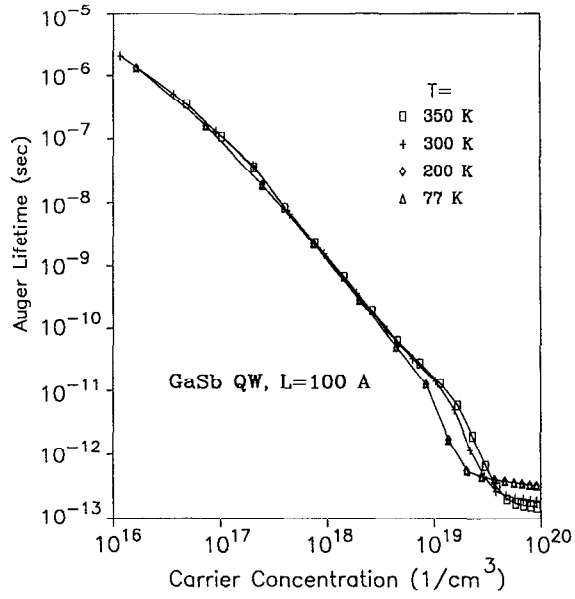

FIG. 6. Calculated band-to-band Auger recombination lifetime in a GaSb QW of width 100 Å at various values of the temperature T. In contrast with the result shown in Fig. 5, it is essentially independent of T.

because of the conservation energy and wave vector. The *CCCH* Auger recombination rate in QW structures is always lower than that in the bulk because of the reduced joint density of states in QW structures at these higher threshold energies.[1] The illustration of this reduction in Figs. 3(b) and 3(d) is not entirely apt because it represents a single carrier; however, the reduction is significant for the joint density of four carriers which takes into account momentum and energy conservation.

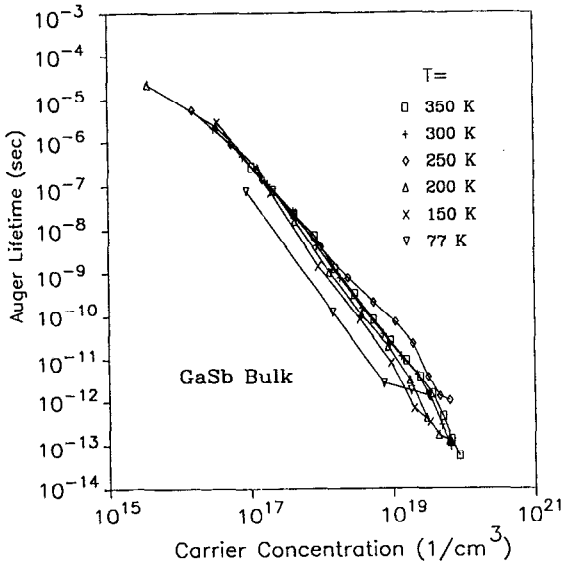

FIG. 5. Calculated band-to-band Auger recombination lifetime in bulk GaSb at various values of the temperature T.

C. Auger recombination in InGaAsP

The illustrations in Figs. 3(b) and 3(d), in which the threshold energies fall above the band edges, also apply to the *CHHS* Auger process in InGaAsP bulk and QW structures, respectively. The Auger recombination rate in the quantum well should presumably exhibit a reduction from the bulk, as is the case for the *CCCH* Auger process in GaAs and HgCdTe. The work reported in Refs. 1 and 6 predict a substantial reduction of the Auger recombination rate in InGaAsP/InP QW lasers. However, one recent measurement of this rate in an InGaAs QW structure[7] shows only a factor-of-3 reduction in comparison with the bulk material, whereas two other measurements show no reduction.[8,9] A reduction of the Auger recombination rate below the radiative recombination rate is important for improving the temperature characteristics of InGaAsP QW lasers. In fact, the picture presented in Sec. III B predicting such a reduction may be too simple, as we now explain.

The Auger process in an InGaAsP QW represents a special case. The discrepancy between the experimental results and the explanation of the density of states reduction given in Sec. III B, as well as the theoretical results given in Refs. 1 and 6, requires us to reexamine Eq. (13). As we can see, each term of the sum in Eq. (13) represents a two-dimensional *CHHS* Auger process involving a set of sublevel bands and has its own threshold. Some of the terms that involve high-energy sublevels may have thresholds at the bottom of these sublevels. Figure 7 shows one example. In most cases, these terms are small because their threshold energies are high. For the InGaAsP QW, although these terms may not have low thresholds, the singularity at $p = 0$ of the matrix element

Downloaded 27 Jan 2002 to 168.122.159.57. Redistribution subject to AIP license or copyright, see http://ojps.aip.org/japo/japcr.jsp

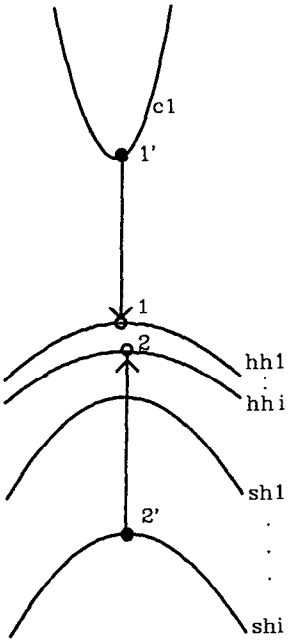

FIG. 7. *CHHS* Auger process in a QW which involves high-energy sublevels. A conduction-band electron 1′ (C), in the sublevel $c1$, recombines with a heavy hole 1 (H) in the sublevel *hh* 1 and excites a heavy hole 2 (H) in the sublevel *hhi* to the spin-split-off band at 2′ (S) in the sublevel *shi*. The threshold energy E_{th} is at the band edge of sublevel *shi*.

$|M|$ has increased order because of the disappearance of some of the zeros at $p = 0$ in the overlap functions. It has been shown[10] that composition-disorder-induced band mixing in ternary and quarternary compounds eliminates the zeros at $p = 0$ in the overlap function $|F_{2,2'}|^2$. The increased order of singularity in $|M|$ enhances these terms so that they may become dominant. The Auger recombination rate in an InGaAsP QW may indeed be increased by the enhancement of these terms, and thereby become comparable with that in the bulk.

CCCH, as well as *CHHH*, Auger recombination rates in a QW structure are not affected by the terms that involve carriers of the high sublevels and have singularities in $|M|$, because the overlap functions in these processes do not change under composition-disorder-induced band mixing. The argument given in Sec. III B is then sufficient.

ACKNOWLEDGMENTS

This work was supported by the Office of Naval Research (N00014-90-J-1536), by the Columbia University Center for Telecommunications Research, and by the Joint Services Electronics Program. We are grateful to Faige Singer and Jill Hacker for useful suggestions.

[1] L. C. Chiu and A. Yariv, IEEE J. Quantum Electron. **QE-18**, 1406 (1982).
[2] A. Sugimura, E. Patzak, and P. Meissner, Surf. Sci. **174**, 163 (1986).
[3] A. Haug, Appl. Phys. Lett. **42**, 512 (1983); M. Takeshima, Phys. Rev. B **25**, 5390 (1982).
[4] A. R. Beatie and P. T. Landsberg, Proc. R. Soc. London Ser. A **239**, 16 (1959).
[5] A. Sugimura, J. Appl. Phys. **51**, 4405 (1980).
[6] A. Sugimura, IEEE J. Quantum Electron. **QE-19**, 932 (1983).
[7] S. Hausser, G. Fuchs, A. Hangleiter, K. Streubel, and W. T. Tsang, Appl. Phys. Lett. **56**, 913 (1990).
[8] E. Zielinski, F. Keppler, S. Hausser, M. H. Pilkuhn, R. Sauer, and W. T. Tsang, IEEE J. Quantum Electron. **QE-25**, 1407 (1989).
[9] B. Sermage, D. S. Chemla, D. Sivco, and A. Y. Cho, IEEE J. Quantum Electron. **QE-22**, 774 (1986).
[10] M. Takeshita, J. Appl. Phys. **49**, 6118 (1978); Y. Jiang, M. C. Teich, and W. I. Wang, J. Appl. Phys. **67**, 2488 (1990).

Downloaded 27 Jan 2002 to 168.122.159.57. Redistribution subject to AIP license or copyright, see http://ojps.aip.org/japo/japcr.jsp